Dynamic Wireless Power Transfer System with an Extensible Charging Area Suitable for Moving Objects

Chen Xu, Yuan Zhuang, Chaoyun Song, Yi Huang and Jiafeng Zhou

***Abstract*—Extensible magnetic resonance coupling-based wireless power transfer (WPT) systems are presented in this paper. A transmitter (Tx) containing an 8-shape loop and two resonators is proposed to construct a bipolar Tx array. A unipolar receiver (Rx) is placed above the Tx perpendicularly to overcome the power null phenomenon. The proposed structure ensures that magnetic flux lines are confined in the vicinity of the Rx, leading to a high power transfer efficiency over a wide range of lateral misalignment distances. Experiments demonstrated that the proposed WPT system can achieve an efficiency of 87% under perfectly aligned operating conditions, and maintain over 70% efficiency from 0 to 30 mm lateral misalignment distances. Based on the proposed Tx module, a single feed Tx array is constructed to further increase the charging area. The power transfer efficiency of a 1×2 array system is between 57.5% and 71.6% without the power null phenomenon. Meanwhile, the concern of heating due to magnetic field leakage can be significantly mitigated. These designs are proved to be very good candidates for dynamic WPT applications.**

***Index Terms*—Dynamic wireless charging, high efficiency, misalignment and wireless power transfer.**

I. Introduction

Wireless power transfer (WPT) technology has been applied to a wide variety of portable consumer electrical, medical, and industrial devices. It has attracted considerable interests and already been proposed for moving objects [1][2]. The WPT systems concerning the charging of moving objects can be divided into three broad categories, namely, static wireless charging [3], dynamic wireless charging (DWC) [4] and Quasi-DWC [5][6].

A review of the state-of-the-art WPT for moving objects indicates that maintaining high-power and high-efficiency when charging a moving object is still a challenge for many DWC systems [7]. DWC transfers the energy using the magnetic coupling between a transmitter and pick-up coils [8]-[9]. The maximum power transfer efficiency (PTE) will only be achieved with perfect alignment, and the efficiency will decrease rapidly with misalignment. For moving objects, power pads that composed of six main components were designed and optimized in [10]. In that work, the maximum efficiency was achieved with a minimum amount of ferrite. To further decrease deployment cost, an ultra-slim S-type power supply rail was proposed in [11]. This power supply rail had a width of only 4 cm. A thin S-shape core was used, and a vertically wound multi-turn coil was placed inside the core. However, the transfer efficiency is still very low in such schemes, because only a small portion of the primary loop contributed to power transfer when the DWC system was working.

By contrast, misalignment is a serious issue for DWC system. Anti-misalignment WPT systems can maintain a high efficiency over a wide range of misalignment conditions [12]. In [13], a dual-loop primary controller was used to regulate primary-side power and current against lateral misalignment. However, only 40% efficiency was achieved in the power null point.

To increase the coupling coefficient between the transmitter and pick-up coils and reduce magnetic flux leakage, bipolar coil topologies with the double-D (DD) shape is widely used for DWC applications of moving objects. However, the power null phenomenon will significantly affect the transferred power level when the Rx moves to the intermediate position between two transmitter coils, causing power pulsation. Hence, the PTE and power pulsation are the main challenges for moving objects charging using DWC technique [14]. In [15], a bipolar coil topology with the double-D (DD) shape and a quadrature coil (Q-coil) was used as the pick-up coil to receive more power in the power null point. However, adding another coil to the Rx would cause other challenges and problems. For instance, the output of the DD coil and the Q-coil are not in phase. As a result, the Q-coil required an individual compensation and rectifier circuit. This results in more power consumption and higher cost in the system. Moreover, shielding of transmission and pick-up coils requires to be considered for a DWPT system. Induction heating phenomena will occur when the operating frequency of the WPT system is up to tens of kHz [16]. Ferrite bars and aluminum plates are usually placed above coils to mitigate those problems [17].

Recently, many 3-D WPT applications are proposed [18]-[20]. Horizontal, vertical and omnidirectional scenarios are studied. These scenarios could raise the concern of end users to meet different requirements of practical applications. In [18], a 3-D WPT system was proposed for laptop applications, where the receiver coil was installed on the screen surface that is perpendicular to the ground plate when the laptop was charged. However, the power transfer efficiency in these studies is

The authors are with the Department of Electrical Engineering and Electronics, University of Liverpool, Liverpool, L69 3GJ, U.K. (e-mail: c.xu12@liverpool.ac.uk;sgyzhua2@163.com;Chaoyun.Song@liverpool.ac.uk ; yi.huang@liverpool.ac.uk; jiafeng.zhou@liverpool.ac.uk).

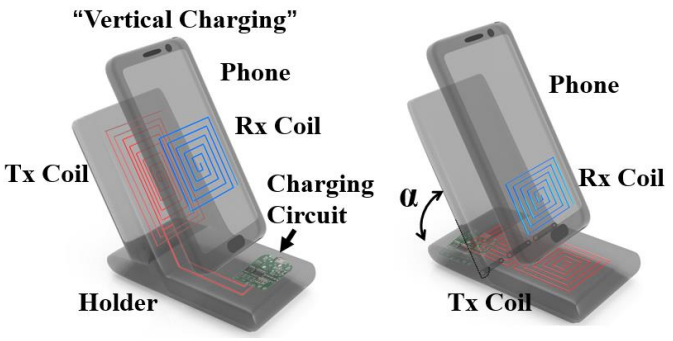

Fig. 1. (a) A typical and (b) the proposed WPT system for portable devices, where the Rx is installed in the phone and Tx is installed in the wireless charging pad.

limited. In [18] and [19], the maximum power transfer efficiencies were 50% and 13%, respectively. In this paper, a WPT system suitable for vertical charging with 87% maximum power transfer efficiency is proposed. It could be a suitable choice for these applications.

In the previous paper [21], a novel WPT system with a perpendicular structure is proposed. The charging module consists of an extensible modularized array to improve the capacity of maintaining high efficiency when the receiver is moving horizontally. In this paper, a mathematical model is derived to calculate the maximum PTE for the proposed WPT system. Meanwhile, the reason why the proposed method can mitigate the power null problem is explained in detail. Another advantage of the proposed system is analyzed and verified in this paper. That is, there is very little magnetic flux leakage beyond the charging area of the proposed WPT system. The induction heating caused by is minimal, and the EMC/EMI performance is also better.

The paper is organized as follows. Section II describes the design and simulation results of the proposed WPT system. Section III presents the experimental results of the proposed system. Finally, conclusions are drawn in Section IV.

II. Operating Principle of the Proposed System

A. Mathematic Modeling and Analysis

"Vertical charging" can be useful in many applications as show in Fig. 1. There are many other potential applications too, such a vertical display unit installed on a horizontal platform or a warehouse robot moving on a fixed track.

To offer greater flexibility when the object to be wirelessly charged is vertical, an 8-shape coil structure was introduced to design resonators in a transmitter [23]. In this work, a WPT system with a perpendicular Tx-Rx charging structure using an 8-shape feed loop is proposed as shown in Fig. 2. The Rx is placed perpendicularly above the center of the Tx. This is defined as the "perfectly aligned" position of the proposed system. For conventional WPT systems, the coils are usually installed in the supporting holder right underneath the charging object as shown in Fig. 1(a). With the proposed design, the supporting part can be a plastic holder only as shown in Fig. 1(b). This would significantly increase the flexibility of the

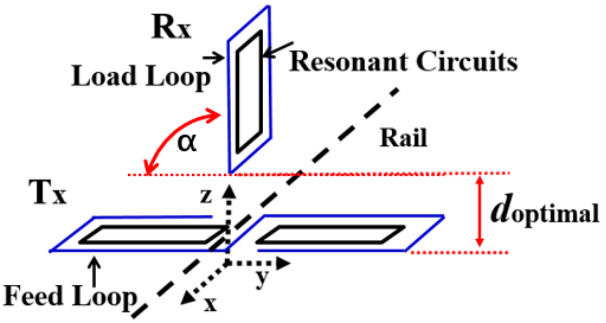

Fig.2. 3-D view of the proposed WPT structure.

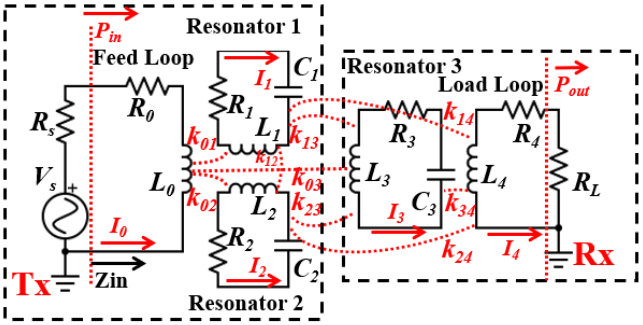

Fig. 3. Simplified schematic of the proposed WPT system.

charger. It can increase the lifespan of the charger as well for mechanical reasons, since the holder can be very light, and it does not have to be connected to the docking base electrically. The holder can be very small, or not needed at all if the device, such as an LED display, can be held up vertically by other means. Furthermore its charging efficiency can be maintained high when the receiver is tilted at different angles, which will be explained in Sect II.B

The Tx has two individual resonators and an 8-shape feed loop. The Rx consists of one resonator and the load loop. The simplified schematic of the proposed WPT system is shown in Fig. 3. According to [24], the reflected impedance Z_{refpq} at the resonant frequency ω_0 from coil q to coil p can be expressed by

$$\begin{bmatrix} Z_{ref01} \\ Z_{ref03} \\ Z_{ref12} \\ Z_{ref13} \\ Z_{ref14} \\ Z_{ref34} \end{bmatrix} = \begin{bmatrix} \frac{(\omega_0 M_{01})^2}{R_1+Z_{ref12}+Z_{ref13}+Z_{ref14}} \\ \frac{(\omega_0 M_{03})^2}{R_3+Z_{ref34}} \\ \frac{(\omega_0 M_{12})^2}{R_2+Z_{ref23}+Z_{ref24}} \\ \frac{(\omega_0 M_{13})^2}{R_3+Z_{ref34}} \\ \frac{(\omega_0 M_{14})^2}{R_L} \\ \frac{(\omega_0 M_{34})^2}{R_L} \end{bmatrix} \quad (1)$$

where M_{pq} is the mutual inductance between the p^{th} and q^{th} coils ($p, q = 0, \ldots, 4$), defined as $M_{pq}= k_{pq}\sqrt{(L_pL_q)}$. M_{01}, M_{02}, M_{12}, M_{13}, M_{23} and M_{34} represent main inductive couplings in the WPT system.

All three resonators in the proposed WPT system are designed with identical parameters $L_1=L_2=L_3$, $R_1=R_2=R_3$ and $C_1=C_2=C_3$. When the Rx is moving along the x-direction, the whole WPT system is symmetrical with respect to the x-z plane as shown in Fig. 4. Therefore, it can be approximated that the mutual inductance between the feed loop and Resonator 1 (M_{01}) equals to the mutual inductance between feed loop and

Resonator 2 (M_{02}). Similarly, M_{13}=M_{23} and M_{14} =M_{24} can be obtained due to symmetry. Then, Z_{ref01}=Z_{ref02}, Z_{ref13}=Z_{ref23} and Z_{ref14}=Z_{ref24}. Thus, the power transfer efficiency of the proposed WPT system can be obtained by the product of the efficiency on each coil/loop can be expressed as (2) as shown next page.

$$\eta_{trn}=\left\{\frac{2Z_{ref01}}{2Z_{ref01}+Z_{ref03}}\left[\frac{Z_{ref13}}{R_1+Z_{ref12}+Z_{ref13}+Z_{ref14}}\frac{Z_{ref34}}{R_3+Z_{ref34}}\right.\right.$$
$$\left.\left.\left(1+\frac{Z_{ref12}}{R_1+Z_{ref12}+Z_{ref13}+Z_{ref14}}\right)+\frac{Z_{ref12}}{R_1+Z_{ref12}+Z_{ref13}+Z_{ref14}}\right.\right.$$
$$\left.\left.\frac{Z_{ref24}}{R_3+Z_{ref21}+Z_{ref23}+Z_{ref24}}\right]+\frac{Z_{ref03}}{2Z_{ref01}+Z_{ref03}}\frac{Z_{ref34}}{R_3+Z_{ref34}}\right\} \quad (2)$$

The output power of the WPT system can be expressed as

$$P_{out}=I_4^2R_L \quad (3)$$

Normaly, P_{out} peaks when R_s=$Re(Z_{in})$. $Re(Z_{in})$ can be calculated according to

$$Re(Z_{in})=R_0+Z_{ref01}+Z_{ref02}+Z_{ref03} \quad (4)$$

When the WPT system is operating at the resonant frequency. The current on each coil/loop can be expressed as

$$\begin{bmatrix}I_0\\I_1\\I_2\\I_3\\I_4\end{bmatrix}=\begin{bmatrix}\frac{V_S}{R_S+R_1+2Z_{ref01}+Z_{ref03}}\\\frac{\omega_0M_{01}I_0+I_1\omega_0M_{12}-I_3\omega_0M_{13}}{R_4+Z_{ref34}}\\\frac{\omega_0M_{01}I_0+I_1\omega_0M_{12}-I_3\omega_0M_{13}}{R_4+Z_{ref34}}\\\frac{2\omega_0M_{13}I_1-I_4\omega_0M_{34}}{R_4+Z_{ref34}}\\\frac{\omega_0M_{34}I_3}{R_L}\end{bmatrix} \quad (5)$$

How different coupling terms in the proposed configuration affect efficiency and power will be analyzed according to (1) and (3). To yield the maximum PTE, the optimal mutual inductances should be

$$M_{13}\approx\frac{\sqrt{\left(\frac{R_2R_3}{\omega_0M_{12}}+\frac{(\omega_0M_{34})^2}{R_L}\right)\sqrt{\frac{(R_1R_2)^2}{(\omega_0M_{12})^2}+\frac{\sqrt{R_0R_1}(\omega_0M_{01})^2}{R_S}}}}{\omega_0} \quad (6)$$

M_{13} (or k_{13}) varies with the lateral displacement Δd, which is the misalignment distance when the Rx is moving along the rail in the x-axis direction. The four main coupling terms need to satisfy R_s=$Re(Z_{in})$ and (7) at the same time to make sure the WPT system can achieve the maximum output power and PTE. Normally, since the range of some coupling terms are limited by applications, the optimal values of other coupling terms should be calculated based on the fixed ones [25]. Parameters of the proposed circuit are listed in Table I in Section III. The calculated optimal values of the main couplings are: k_{01}=0.247, k_{34}=0.33, k_{12}=0.04 and k_{13}=0.077.

Analytically, the relationship among the coupling coefficient k_{23}, d and Δd can be expressed using Neumann formula [26], numerical iterations [27] and Biot-Savart law [28]. In this study, Computer Simulation Technology (CST) and Maxwell, the software packages based on high precision Finite Element Analysis, are used to evaluate the mutual inductances, coupling coefficients and optimal distances for convenience. The maximum PTE is achieved if the Rx is placed $d_{optimal}$ above the Tx when they are aligned, and α is misalignment angle between Rx and line perpendicularly with Tx. The operating frequency is selected to be 13.56 MHz, which is the resonant frequency of all resonators in the system. The value of the external capacitors can be calculated according to $f=\frac{1}{2\pi\sqrt{LC}}$.

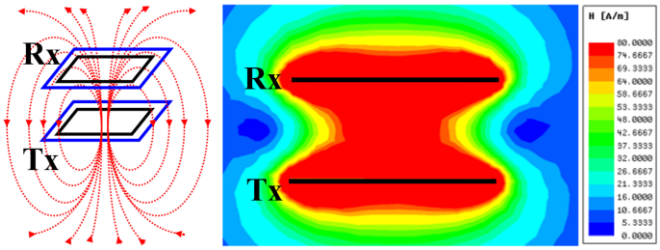

Fig. 4. Magnetic field distribution of the four-coil WPT system.

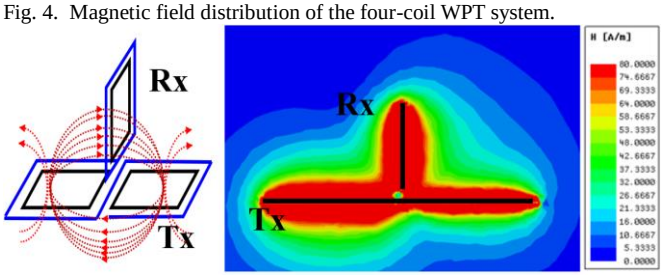

Fig. 5. Magnetic field distribution of the proposed WPT system.

The cross-coupling between Tx side coils is M_{12}. The critical value of M_{12} can be calculated according to (7) as

$$M_{12}\approx\frac{R_1R_2}{\sqrt{\omega_0^2\left(\frac{M_{13}}{M_{34}}\right)^4R_L^2-\frac{\sqrt{R_0R_1}\omega_0^4M_{01}^2}{R_S}}}+\frac{R_1R_2}{\frac{\sqrt{R_S}M_{13}^2\omega_0^2}{(R_0R_1)^{0.25}M_{01}}\frac{(\omega_0M_{34})^2}{R_L}} \quad (7)$$

It is noted that there is a dip near the resonant frequency when the cross coupling is relatively strong. The dip will disappear when k_{12} is smaller than the critical value. R_L and M_{13} need to satisfy (7) to achieve the best performance of the proposed WPT system. In this study, a VNA was used to measure the PTE of the WPT system. For convenience, the input and output impedances were set to 50 Ω. Then, M_{13} was optimized to achieve the optimal performance.

B. The Proposed WPT System

As shown in Fig. 5, the Tx in a conventional four-coil WPT system is unipolar. The flux lines leave the top surface and enter the bottom surface of the Tx, and vice versa periodically. For the Tx in the proposed WPT system, due to the use of the 8-shape feed loop, the current goes in the clockwise direction in one part and in the anti-clockwise direction in the other part. This results in a bipolar structure for the Tx. The top surface of the Tx has both north pole and south pole as shown in Fig. 6. Magnetic flux lines leave the top region of one coil in the Tx and enter the top region of the other coil in the Tx through the Rx.

Another common issue associated with WPT is the induction-heating phenomenon [16]. Compared with the WPT system using a unipolar Tx, the magnetic field is confined to a small space above the Tx in the proposed WPT system. This would significantly reduce the heat induced by magnetic field leakage to any metal parts close to the WPT system. This makes

the proposed WPT system even more suitable for DWC of moving objects. The robustness of the proposed WPT system maintaining high efficiency against lateral displacement Δd was analyzed, where Δd was varied from 0 to 70 mm with a step of 10 mm. As shown in Fig.6 (a) and (c), the real part of the input impedance at the resonant frequency declined very slowly when the misalignment is from 0 to 25 mm. The imaginary part of the input impedance for different Rx positions against frequency was shown in Fig.7 (b). The proposed WPT system can maintain high efficiency and output power against lateral displacement.

Meanwhile, the charging efficiency can be maintained high when the receiver is tilted at different angles as shown in Fig. 7. The mutual coupling terms M_{13}, M_{23}, and PTE are simulated, where α is varied from 0 to 90 degrees with a step of 5 degrees. According to Fig. 7, M_{13} increases when Rx is titled from its perfect aligned position to Resonator 1, M_{23} decreases slowly at the same time. As a result, the sum of the mutual inductances between all Tx resonators and the Rx, $ABS(M_{13}+M_{23})$, has very little changes when the Rx is tilted between +/- 40º. Thus, the whole WPT system will have a stable PTE against the tilted angle of the Rx. This feature is especially beneficial if the device is being used when charging, since a user can tilt the device at different angles very easily without degrading efficiency.

C The Proposed WPT System for DWC

Bipolar coil topology is widely used for DWC of moving object applications. It not only increases the coupling coefficient between the Tx and Rx, but also reduces magnetic flux leakage [17]. However, eliminating the power null phenomenon is still a main challenge. A typical DWC system with bipolar coil topology is shown in Fig. 8. Parameters of the simulation circuit are listed in Table I in Section III. The structures of the Tx and Rx are the same when using the DD type of bipolar coils. Two Txs are placed below the Rx for DWC. When the Rx moves along the two Txs, in the middle point the net magnetic flux on the Rx becomes zero as shown in Fig. 8. At this point, there is no power transferred from the Tx to the Rx.

The sum of mutual inductances between all Tx coils and the Rx can be used to evaluate the total power transferred in a multi-Tx DWC system [29]. The mutual inductance M_{RTi} between the i_{th} Tx (i=1,2) and the Rx can be obtained by simulation using the software package Maxwell. The variation of the mutual inductance with respect to distance is shown in Fig. 9. The absolute value of the sum of M_{RT1} and M_{RT2} is denoted as $ABS(M_{RT1}+M_{RT2})$. It can be seen that M_{RT1} varies from a high positive value to a negative value when the Rx moves along the Txs. M_{RT2} has a symmetrical varying profile with M_{RT1}. Hence, $ABS(M_{RT1}+M_{RT2})$ fluctuates from the maximum to zero and back to the maximum. When $ABS(M_{RT1}+M_{RT2})$ reaches zero, no power is transferred in the WPT system.

One conventional method to eliminate the power null phenomenon is to add another rectangular coil (Q-coil) to the Rx, which composes a DDQ type Rx. When the Rx moves to the null power point, the DD coils stop receiving power from the Tx. The net magnetic flux on the Q-coil reaches its maximum. Conversely, the net magnetic flux on the Q-coil decreases to zero when the Rx moves to the aligned position, where the DD coils on the Rx produce the maximum power. Therefore, the DDQ design can mitigate the power null phenomenon and

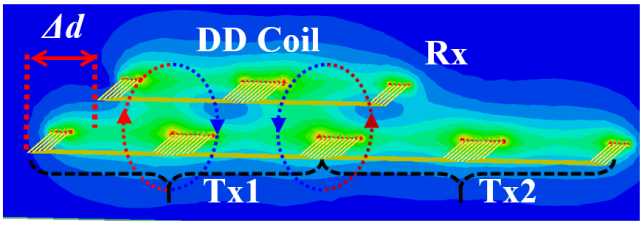

Fig. 8. Diagram to illustrate the power null phenomenon. This is the 3-d view of a WPT system with DD coils when the Rx is placed on the null power point. The magnetic flux lines are highlighted to describe that the net flux on the Rx is zero at this point.

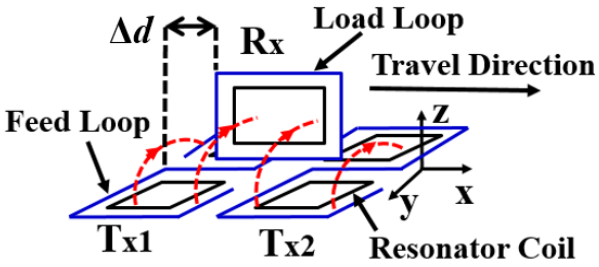

Fig. 9. Diagram of the proposed WPT system.

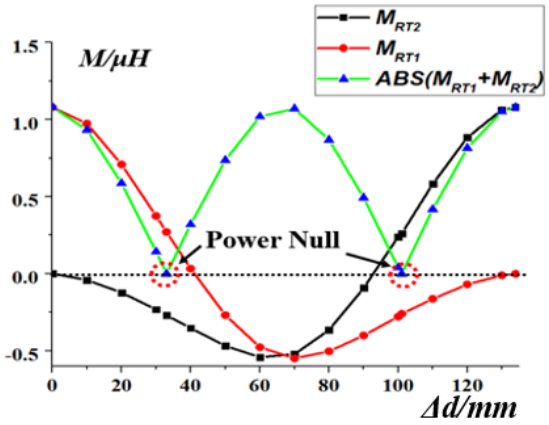

(a)

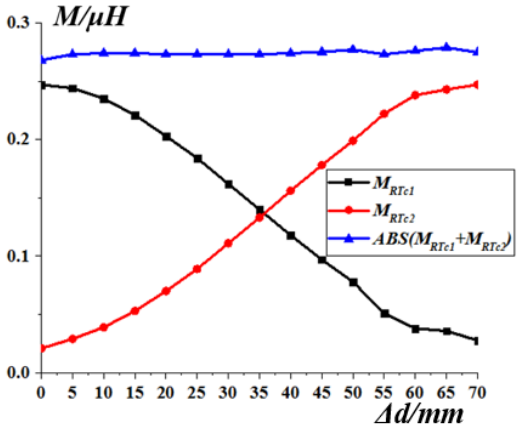

(b)

Fig. 10. The mutual inductance against Δd of the WPT systems using (a) the DD type of coils and (b) the proposed WPT system.

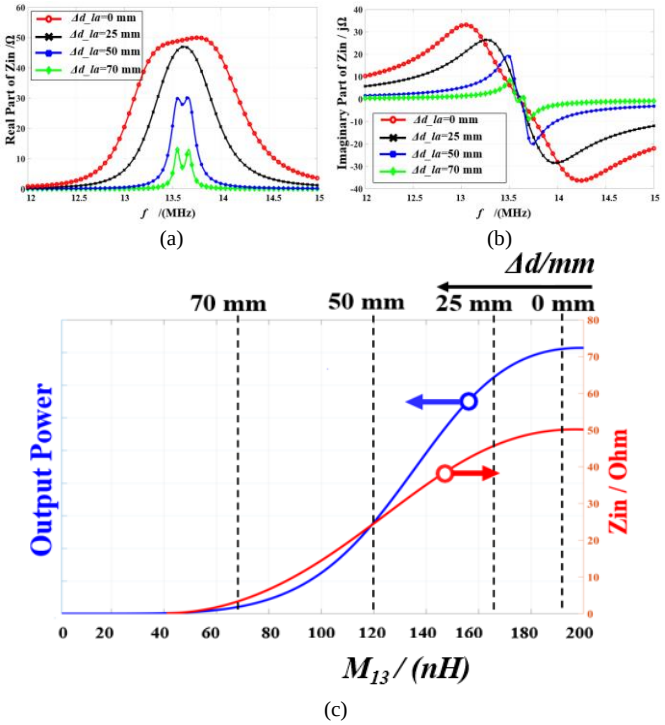

Fig.6. (a) The real part of the input impedance of the WPT system and (b) the imaginary part of the input impedance for different Rx positions (lateral displacement Δd) against frequency. (c) The real part of the input impedance and output power against M_{13} and lateral displacement Δd.

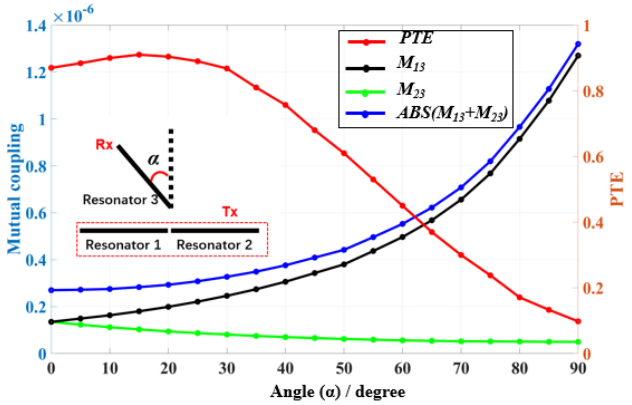

Fig.7. PTE and mutual coupling of the proposed system against angular misalignment α.

reduce the power fluctuation. However, adding another coil to the Rx would cause other challenges and problems. Firstly, the manufacturing cost would be increased. Secondly, the Q-coil needs to be optimized carefully. Study [30] has focused on this research topic. It makes the whole WPT system much more complex. Moreover, due to that the reflected impedance from the Q-coil to the Tx is different from that of the DD coil, the output of the DD coil and the Q-coil are not in phase. As a result, the Q-coil required an individual compensation and rectifier circuit. This results in more power consumption in the system and lower PTE.

The proposed 1×2 DWC system is shown in Fig. 7(d). Parameters of the simulation circuit are listed in Table I in Section III. The Rx in the proposed WPT system is placed perpendicularly with the Tx and it moves along the x-axis.

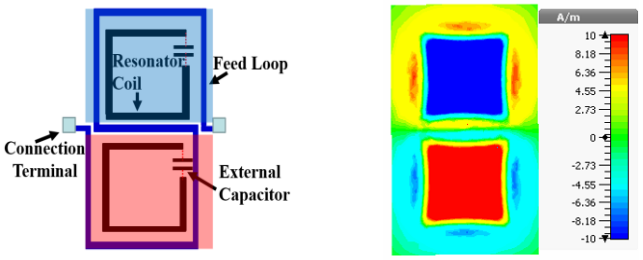

Fig. 11. (a) Diagram of the extensible module. (b)Magnetic field distribution on the surface of the module.

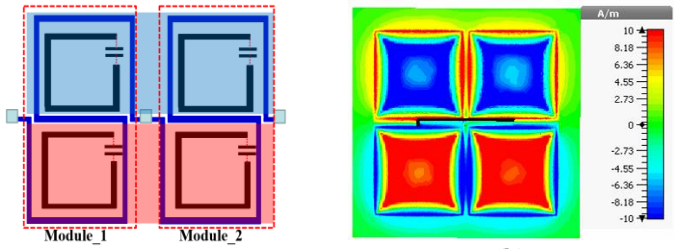

Fig. 12. (a) Diagram of a 1×2 Tx array. (b) Magnetic field distribution on the surface of the 1×2 Tx array.

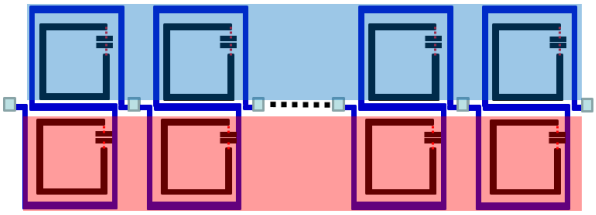

Fig. 13. Diagram of a 1×n Tx array.

When the Rx moves along the travel direction, flux lines go through it from the one side to the other side. Hence, the net magnetic flux on the Rx would not be zero. These mutual inductances are calculated using Maxwell and shown in Fig. 10. The mutual inductance between the Rx and the i_{th} Tx (i =1, 2) is denoted as M_{RTci}. The absolute value of the sum of M_{RTc1} and M_{RTc2} is denoted as $ABS(M_{RTc1}+M_{RTc2})$. It can be found that M_{RTc1} and M_{RTc2} are always in-phase as shown in Fig.10.

Therefore, the power null phenomenon is very significantly mitigated in the proposed WPT system. Compared with the simulation results in Fig. 9, $ABS(M_{RTc1}+M_{RTc2})$ varies in a much smaller range, which means the output power fluctuation can be drastically reduced in the proposed WPT system. The proposed WPT system maintains the advantage of using bipolar coils by confining magnetic flux lines in a smaller space, thereby reducing the concern about field leakage.

D The Proposed Extensible WPT System

To further increase the wireless charging area, a multi-transmitter structure can be constructed. However, a traditional WPT system with multiple transmitters requires that the transmitters are synchronized in frequency, phase, and amplitude [31]. This results in a complicated control mechanism and structure. Even though all transmitters were synchronized as required, the WPT system would still have

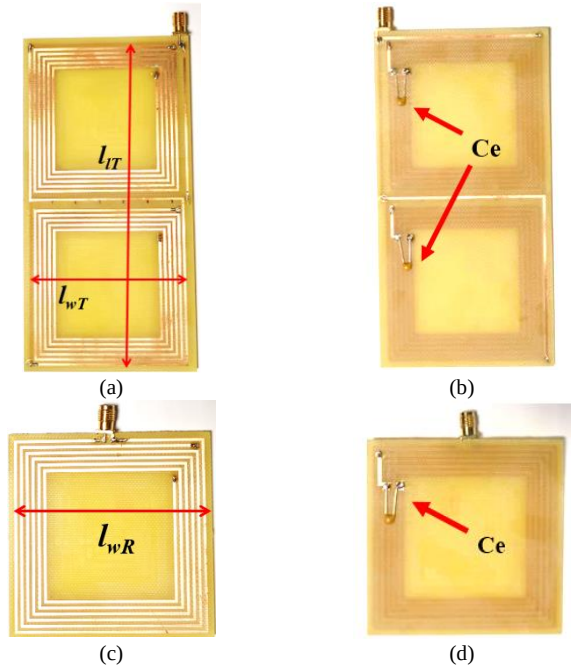

Fig. 14. Photographs of (a) the top layer of the fabricated Tx module; (b) the bottom layer of the fabricated Tx module; (c) the top layer of the fabricated Rx and (d) the bottom layer of the fabricated Rx.

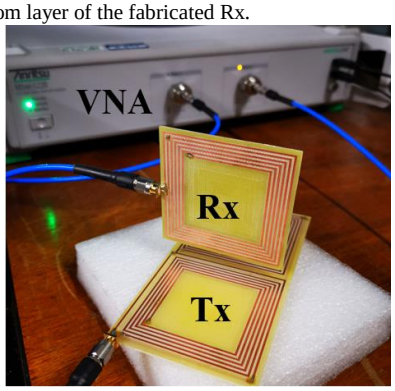

Fig. 15. The experimental setup of the proposed WPT system with a single Tx module.

TABLE I
PARAMETERS OF THE FABRICATED CIRCUIT

Parameters	Value	Unit
Turns of resonator coil	5	NA
Copper Height h_c	0.035	mm
Track Width w_c	1	mm
Space Between Tracks l_s	1	mm
widths of the Tx l_{wT}	63	mm
widths of the Rx l_{wR}	63	mm
length of the Tx l_{lT}	131	mm
Capacitance of external capacitor (Ce)	60	pF
Self-inductance of resonator coil	2.320	μH
Self-inductance of feed loop	0.911	μH
Self-inductance of load loop	0.544	μH
Self-inductance of DD-coil	6.808	μH

power null phenomena as introduced above.

A study in [32] used a planar array for the Tx to increase the charging area. The planar array of a conventional magnetically coupled resonance (MCR)-WPT system has a fixed feed loop to drive resonators in the Tx [33]. Using the proposed structure, a modularized array can be constructed with simpler transmitter connections.

Fig. 11 (a) shows the proposed bipolar Tx as introduced in Section II.A, which can be used as an extensible module. When an AC power source is connected between the two connection terminals, the current flowing through the feed loop can generate magnetic field of opposite directions on the two resonators of the module. If the north pole is generated in the red region, the south pole will be generated in the blue region. The magnetic field strength H on the surface of the module is simulated by using CST and shown in Fig. 11 (b).

The feed loops in the modules can be connected in series to form a planar 1×n Tx array. In the simplest scenario when only two modules are needed, connection of the two modules is shown in Fig. 12(a). The feed loops in Module 1 and Module 2 are connected through the connection terminals. Such connections ensure that the current flowing through the two feed loops has the same direction in the two modules. Therefore, the poles in the red region are the same, and are opposite from those in the blue region. The simulated magnetic field distribution is shown in Fig. 12(b).

According to the same principle, the proposed extensible WPT can enlarge the charging area further by increasing the number of modules in the Tx. Fig 13 demonstrates a 1×n Tx array which can be used in a DWC system. As long as the Tx modules are in phase, synchronization is not needed. The proposed WPT system can generate a stable magnetic field on the surface of the Tx, which ensures that the WPT system will continue to work with high efficiency when the Rx is moving along the symmetrical line.

III. EXPERIMENTAL VALIDATION

The proposed WPT system with a single charging module was fabricated on an FR4 printed circuit board (PCB) with a double layer structure as shown in Fig. 14. Inductive coils and feed/load loops were constructed by copper tracks on the PCB, whose thickness and width are denoted as h_c and w_c, respectively. The feed loop was fabricated on both layers of the PCB to form an "8" shape, as shown in Fig. 14 (a) and (b). The load loop for the Rx was fabricated on the top layer as shown in Fig. 14 (c). All resonators in the proposed WPT system had the same dimensions. They were fabricated on one side of the PCB connected with external capacitors soldered on the other side to form resonators. Parameters of the fabricated circuit are listed in Table I. The experimental setup of the proposed WPT system with a single Tx module is shown in Fig. 15. The Rx was placed perpendicularly above the Tx module, so that they were aligned with each other.

An Anritsu MS46322B vector network analyser (VNA) was used to measure the PTE of this WPT system. S-parameters were utilized as an indicator for power transfer performance of the WPT system. $|S_{21}|^2$ can be used to evaluate the efficiency of the WPT system. In the aligned condition as shown in Fig. 15, the maximum efficiency can be achieved with a charging height of 5 mm, where S_{11} = -26.8 dB and S_{21} = -0.6 dB at the operating frequency of 13.56 MHz. The maximum efficiency is calculated to be 87.1%. The conventional four-coil WPT system was fabricated for comparison, whose Tx and Rx had the same design as the Rx in the proposed WPT system. The maximum

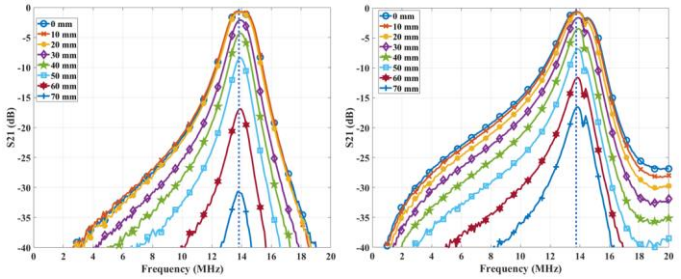

(a) (b)

Fig. 16. Measured results of (a) the conventional and (b) the proposed WPT system against lateral displacement.

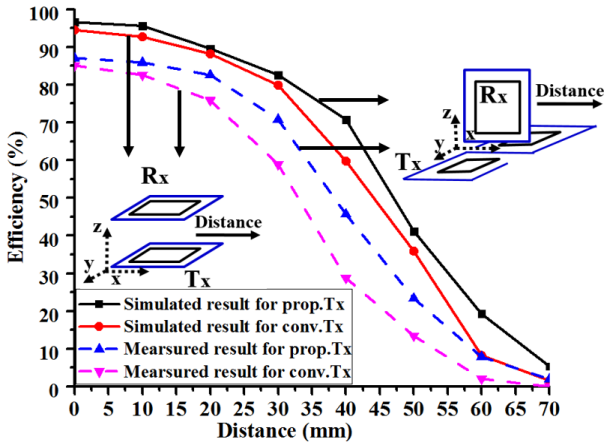

Fig. 17. WPT efficiencies of the systems with the proposed single-module Tx and the conventional Tx.

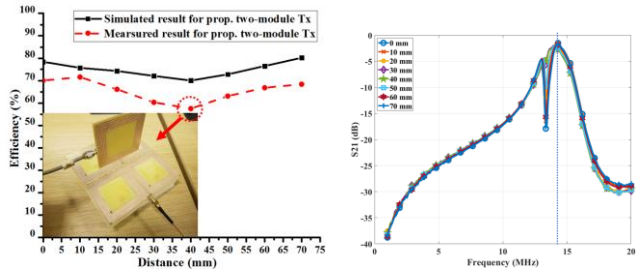

(a) (b)

Fig. 18. Measurement results of (a) WPT efficiency as a function of the misalignment distance of the proposed WPT system with a 1×2 array Tx and (b) S_{21} against the misalignment distance.

PTE achieved was 85%.

The robustness of the proposed WPT system maintaining high efficiency against lateral displacement was measured. The misalignment was varied from 0 to 70 mm with a step of 10 mm. At each distance, the S-parameters were measured to calculate the efficiency.

Fig. 16 (b) shows the measured efficiency as a function of the Δd. The efficiency declined slowly when the misalignment is from 0 to 25 mm. From 25 to 35 mm, there is still strong and consistent coupling existing between the Rx and Tx and the efficiency was still over 60%. After a misalignment distance of 35 mm, the efficiency dropped rapidly, because the overlapping area of the Rx and Tx was less than half of the maximum physical size of the Tx or Rx. Therefore, no strong coupling existed between the Rx and Tx after this point. The designed WPT system had over 70% efficiency when the misalignment distance varied from 0 to 30 mm which was 42.9% of the width of the Tx or Rx.

The performance of the proposed WPT system was also compared with the conventional WPT system with a four-coil structure shown in Fig. 16 (a). For fair comparison, the

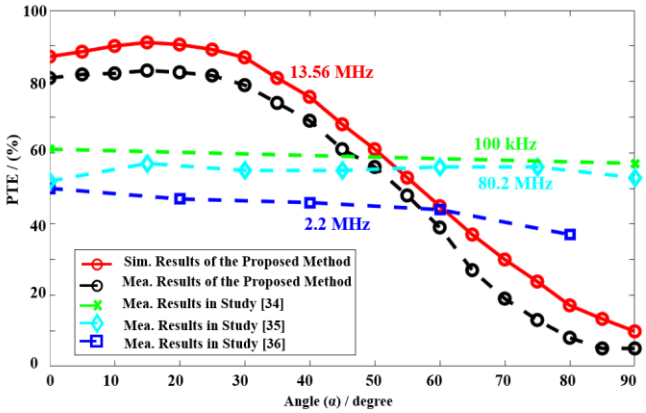

Fig. 19. Measured results of the proposed WPT system against angular misalignment. The performance is compared with other work.

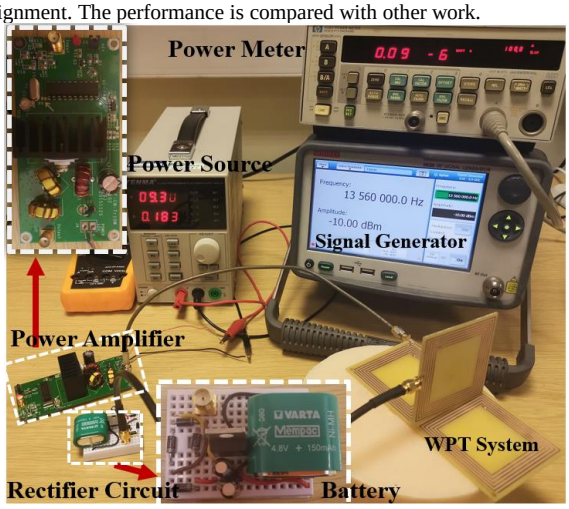

Fig. 20. Experimental setup of the proposed WPT system when charging a battery load.

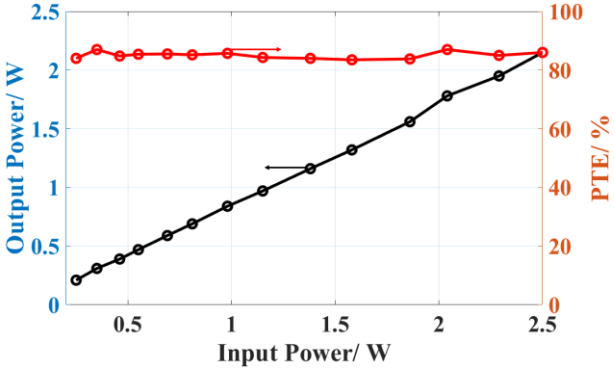

Fig. 21. Measured results of the proposed WPT system when charging a battery.

conventional WPT system was fabricated on a PCB with the same overall dimensions as the proposed one.perfectly aligned with Module 1 to the position where the Rx is The experimental setup for the proposed extensible WPT system is shown in Fig. 18(a). The Tx is extended to a 1×2 array with connections described in Section II.C. The two Tx modules with a separation distance of 1 mm were connected in

series to form the Tx. The Rx remained unchanged and was placed above the Tx at the optimal distance. The PTE versus the lateral misalignment distance Δd is shown in Fig. 18(b). The performance of the extensible WPT system with a moving Rx is measured. The lateral misalignment distance was changed with an increment of 10 mm from the position where the Rx is aligned with Module 2. The efficiency decreases very slowly when the displacement of the Rx was less than the 40 mm. After a lateral displacement of 40 mm, the coupling between the Rx and Module 2 in the Tx became stronger. This leads to an increasing efficiency for the distance from 40 mm to 70 mm. The efficiency increases to the peak again when the Rx is perfectly aligned with Module 2 in the Tx. This process would repeat when the Rx is moving further towards the next module.

Fig. 18 (b) shows the measured S_{21} of the 1×2 array system with respect to the lateral displacement. Compared with the results shown in Fig. 16, the S_{21} is much more stable so that the proposed extensible WPT system has a much better performance against lateral displacement. The WPT system with a 1×2 Tx array can achieve 71.6% maximum efficiency when the Rx was aligned with Module 1 or Module 2. The minimum efficiency of the proposed WPT systems is better than 57% at all positions. It validates that the proposed WPT system can significantly reduce the output fluctuation and overcome the power null phenomenon. It is noted that there is a "valley" near the resonant frequency. This is because two charging modules are place close to each other so that the 1×2 Tx array has another self-resonant frequency near the resonant frequency. Since usually WPT systems are only operated at the system resonant frequency, this "valley" would not affect the performance of the system.

The simulated and measured PTEs versus angular misalignment are shown in Fig. 19. The angular misalignment α was changed with an increment of 5 degrees from its prefect aligned position. The efficiency changes very slowly and the value is over 75% when α is in the range of ±40 degrees. The simulated and measured results are in good agreement. These results are compared with other angular misalignment tolerant WPT systems [34] - [36]. Both Tx's in study [34] and [35] have a spherical shape, which results in a complicated structure and limited applications. In study [36], there are two coils in the Rx and they are orthogonal with each other, which is not very suitable for portable devices. Both Tx and Rx in the proposed design have a planar structure, which is much more suitable for practical applications.

Experimental setup of the proposed WPT system charging a battery load is shown in Fig. 20. A power amplifier was used to generate input power at 13.56 MHz for the WPT system. A rectifier circuit was added between the Rx and the battery load. A 4.8 V, 150 mAh rechargeable battery was charged. The proposed WPT system was measured when the Rx was placed in its perfectly aligned position. The PTE was defined as the ratio of battery charging power to the output power of the power amplifier. The measured efficiency and output power as a function of the input power is shown in Fig. 21. The output power and input power have a good linear relationship. The PTE is stable when the input power was changed from 0.25 W to 2.5 W. Because the rated current of the battery is 500 mA, the experiment test was limit to 2.5 W. Higher power is achievable if the coils are constructed accordingly [37].

The proposed WPT system demonstrates a technology with great potential for many practical applications. For static wireless charging applications, the proposed design can be utilized to charge devices such as phones, tablets, LED displays, where these devices can be placed vertically to the chargers. For dynamic wireless charging applications, the proposed extensible WPT system is suitable for charging mobile robots when they move along a fixed trace or a sliding rail, such as carrier robots in a smart warehouse.

IV. Conclusion

In conclusion, an extensible WPT system with a bipolar Tx and a perpendicular Rx-Tx structure has been proposed in this paper. An 8-shape feed loop and two resonators were used to construct a bipolar Tx module. The Tx module can be easily extended to a bipolar Tx array. This feature enables the proposed WPT system to have an excellent extensibility.

The output power fluctuation can be significantly reduced using this bipolar Tx array. The proposed WPT system can overcome the power null phenomenon very effectively compared with the method of using DDQ coils. Since the unipolar Rx and bipolar Tx are placed perpendicularly with each other, the magnetic flux lines are mainly confined in the vicinity of the WPT system. As demonstrated by experiment, the proposed extensible WPT system can achieve a high efficiency of 57% - 71.6% when an Rx moves along a two-module Tx.

The proposed design will also significantly minimize the effect of surrounding metal parts on the WPT system, since the magnetic field is mainly distributed in the vicinity of the charging area. The proposed WPT system presents a technology with great potential for many practical designs.

References

[1] S. Li and C. C. Mi, "Wireless power transfer for electric vehicle applications," *IEEE Journal of Emerging and Selected Topics in Power Electronics*, vol. 3, no. 1, pp. 4-17, 2015.

[2] Z. Ali, S.Vaez-Zadeh, and A. Babaki. "A Dynamic WPT System With High Efficiency and High Power Factor for Electric Vehicles." in *IEEE Transactions on Power Electronics*, vol.35, no.7, pp. 6732-6740, 2020

[3] M. Zhang, *et al*, "The charging control and efficiency optimization strategy for WPT system based on secondary side controllable rectifier." *IEEE Access*, (Early Access Article), 2020.

[4] P. Darvish, S. Mekhilef, and H. A. Illias, "A Novel S-S-LCLCC Compensation for Three-Coil WPT to Improve Misalignment and Energy Efficiency Stiffness of Wireless Charging System," in *IEEE Transactions on Power Electronics.* (Early Access Article), 2020.

[5] S. Lukic and Z. Pantic, "Cutting the cord: Static and dynamic inductive wireless charging of electric vehicles," *IEEE Electrification Magazine*, vol. 1, no. 1, pp. 57-64, 2013.

[6] L. Patnaik, *et al*, "Wireless opportunity charging as an enabling technology for EV battery size reduction and range extension: Analysis of an urban drive cycle scenario," in *2018 IEEE PELS Workshop on Emerging Technologies: Wireless Power Transfer (Wow)*, pp. 1-5, 2018.

[7] A. Ahmad, M. S. Alam and R. Chabaan, "A comprehensive review of wireless charging technologies for electric vehicles," *IEEE Transactions on Transportation Electrification*, vol. 4, no. 1, pp. 38-63, 2018.

[8] T. Fujita, T. Yasuda and H. Akagi, "A dynamic wireless power transfer system applicable to a stationary system," *IEEE Trans. Ind. Appl*., vol. 53, no. 4, pp. 3748-3757, 2017.

[9] R. Ainur, et al. "Precise analysis on mutual inductance variation in dynamic wireless charging of electric vehicle." *Energies* vol. 26, no. 3, 2018

[10] M. Budhia, G. A. Covic and J. T. Boys, "Design and optimization of circular magnetic structures for lumped inductive power transfer systems," *IEEE Transactions on Power Electronics*, vol. 26, no. 11, pp. 3096-3108, 2011.

[11] S. Y. Choi et al, "Ultraslim S-type power supply rails for roadway-powered electric vehicles," *IEEE Transactions on Power Electronics*, vol. 30, no. 11, pp. 6456-6468, 2015.

[12] S. Ding, W. Niu, and W. Gu, "Lateral Misalignment Tolerant Wireless Power Transfer With a Tumbler Mechanism", *Access IEEE*, vol. 7, pp. 125091-125100, 2019.

[13] R. Tavakoli and Z. Pantic, "Analysis, Design, and Demonstration of a 25-kW Dynamic Wireless Charging System for Roadway Electric Vehicles," *IEEE Journal of Emerging and Selected Topics in Power Electronics*, vol. 6, no. 3, pp. 1378-1393, 2018.

[14] X. Dai, J. Jiang and J. Wu, "Charging Area Determining and Power Enhancement Method for Multi-Excitation Unit Configuration of Wirelessly Dynamic Charging EV System," *IEEE Trans. Ind. Electron*., 2018.

[15] A. Zaheer et al, "Investigation of multiple decoupled coil primary pad topologies in lumped IPT systems for interoperable electric vehicle charging," *IEEE Transactions on Power Electronics*, vol. 30, no. 4, pp. 1937-1955, 2015.

[16] J. Acero et al, "Analysis of the Mutual Inductance of Planar-Lumped Inductive Power Transfer Systems," *IEEE Transactions on Industrial Electronics* vol. 60, no. 1, 2013.

[17] M. Kavitha, P. B. Bobba and D. Prasad, "Effect of coil geometry and shielding on wireless power transfer system" *2016 IEEE 7th Power India International Conference (PIICON)*, 2016

[18] H. Lee, et al. "MR-WPT with reconfigurable resonator and ground for laptop application." *IEEE Microwave and Wireless Components Letters*, vol.28, no.3, pp. 269-271, 2018.

[19] P. Alex, et al. "Design of a Miniaturized Omni-Directional RF-to-dc IR-WPT." *2018 IEEE Wireless Power Transfer Conference (WPTC)*. IEEE, 2018.

[20] Alshhawy, et al. "Separation-Misalignment Insensitive WPT System Using Two-Plane Printed Inductors." *IEEE Microwave and Wireless Components Letters*, vol.29, no.10, pp. 683-686, 2019

[21] C. Xu, et al, "Charging Area Extensible Wireless Power Transfer System with an Orthogonal Structure" *In Wireless Power Week 17-21 June LONDON*. 2019,

[22] Y. Zhang, Z. Zhao and K. Chen, "Frequency splitting analysis of magnetically-coupled resonant wireless power transfer," in *Energy Conversion Congress and Exposition (ECCE)*, 2013 IEEE, 2013, pp. 2227-2232.

[23] C. Xu, et al, "Multi-coil high efficiency wireless power transfer system against misalignment," in *2018 IEEE MTT-S International Wireless Symposium (IWS)*, 2018.

[24] Y. Zhang, "Key Technologies of Magnetically-Coupled Resonant Wireless Power Transfer"; *Springer: Singapore*, 2017.

[25] J. Kim, W. Choi and J. Jeong, "Loop switching technique for wireless power transfer using magnetic resonance coupling," *Progress in Electromagnetics Research*, vol. 138, pp. 197-209, 2013.

[26] S. Raju et al, "Modeling of mutual coupling between planar inductors in wireless power applications," *IEEE Transactions on Power Electronics*, vol. 29, no. 1, pp. 481-490, 2014.

[27] S.I. Babic and C. Akyel, "New analytic-numerical solutions for the mutual inductance of two coaxial circular coils with rectangular cross section in air" *IEEE Transactions on Magnetics*, vol. 42, no. 6, pp. 1661-1669, 2006.

[28] R. Ravaud et al, "Cylindrical Magnets and Coils: Fields, Forces, and Inductances," *IEEE Transactions on Magnetics* vol. 46, no. 9, pp. 3585-3590, 2010.

[29] Q. Zhu, at el, "Applying LCC Compensation Network to Dynamic Wireless EV Charging System," in *IEEE Transactions on Industrial Electronics*, vol. 63, no. 10, pp. 6557- 6567, Oct. 2016.

[30] C. C. Mi, at el, "Modern Advances in Wireless Power Transfer Systems for Roadway Powered Electric Vehicles," in *IEEE Transactions on Industrial Electronics*, vol, 63, no. 10, pp. 6533-6545, 2016.

[31] R. Johari, J. V. Krogmeier and D. J. Love, "Analysis and practical considerations in implementing multiple transmitters for wireless power transfer via coupled magnetic resonance," *IEEE Trans. Ind. Electron.*, vol. 61, no. 4, pp. 1774-1783, 2014.

[32] F. Jolani, Y. Yu and Z. Chen, "A planar magnetically-coupled resonant wireless power transfer using array of resonators for efficiency enhancement," in Microwave Symposium (IMS), 2015 *IEEE MTT-S International*, 2015, pp. 1-4.

[33] Z. Liu, et al, "A Shape-Reconfigurable Modularized Wireless Power Transfer Array System for Multi-Purpose Wireless Charging Applications," *IEEE Transactions on Antennas and Propagation*, 2018.

[34] Z. Zhang and B. Zhang, "Angular-Misalignment Insensitive Omnidirectional Wireless Power Transfer," in *IEEE Transactions on Industrial Electronics*, vol. 67, no. 4, pp. 2755-2764, April 2020.

[35] D. Liu, H. Hu and S. V. Georgakopoulos, "Misalignment Sensitivity of Strongly Coupled Wireless Power Transfer Systems," in *IEEE Transactions on Power Electronics*, vol. 32, no. 7, pp. 5509-5519, July 2017

[36] J. P. W. Chow, N. Chen, H. S. H. Chung and L. L. H. Chan, "An Investigation Into the Use of Orthogonal Winding in Loosely Coupled Link for Improving Power Transfer Efficiency Under Coil Misalignment," in *IEEE Transactions on Power Electronics*, vol. 30, no. 10, pp. 5632-5649, Oct. 2015,

[37] Z. Liu, et al. "Planar magnetically-coupled resonance wireless power transfer systems using array of coil resonators." *2016 IEEE MTT-S International Wireless Symposium (IWS)*. IEEE, 2016.